

## The Peculiar Properties of Cold Quasars

---

**Allison Kirkpatrick,<sup>a,\*</sup> Brandon Coleman,<sup>a</sup> Claire Cook<sup>a</sup> and Anika Goel<sup>b</sup>**

<sup>a</sup>*Department of Physics and Astronomy, University of Kansas,  
1251 Wescoe Hall Drive, Lawrence, KS 66045, USA*

<sup>b</sup>*Department of Astronomy, Indiana University,  
727 East 3rd Street, Bloomington, IN 47405, USA*

*E-mail:* [akirkpatrick@ku.edu](mailto:akirkpatrick@ku.edu)

All massive galaxies host a supermassive black hole at their centers. Some of these supermassive black holes go through growth spurts and feeding frenzies that can greatly impact their host galaxies, possibly even terminating all nearby star formation. In this talk, I will explore a new class of quasars, cold quasars, which are some of the most luminous accreting black holes in the universe, and yet, surprisingly, their host galaxies have star formation rates of  $1000 M_{\odot}/\text{yr}$ , casting doubt on whether black hole feedback impacts star formation at all. I will discuss how cold quasars are an anomaly in the current understanding of quasar formation.

*Multifrequency Behaviour of High Energy Cosmic Sources XIV (MULTIF2023)  
12-17 June 2023  
Palermo, Italy*

---

\*Speaker

## 1. Introduction

Observational evidence indicates that almost every large galaxy hosts a supermassive black hole at its center. These black holes are tied to the evolution of their host galaxies, as evidenced by the tight relation between a galaxy’s stellar mass ( $M_*$ ) and black hole mass ( $M_\bullet$ ) that persists over several orders of magnitude in the local universe [1]. Further, the peak of stellar mass buildup (traced through the star formation rate density) and black hole mass buildup (traced through the black hole accretion rate density) occurred concurrently around  $z \sim 2$ , arguing for co-evolution over cosmic time [2]. The physical mechanism linking the two phenomena remains uncertain, although feedback emanating from near the supermassive black hole is one possible culprit.

A supermassive black hole that is accreting material is referred to as an active galactic nucleus (AGN); these objects are often identified through their bright X-ray emission  $L_X > 10^{42}$  erg/s. A quasar is an extremely luminous active galactic nucleus (typically,  $L_X > 10^{44}$  erg/s). Canonically, the formation of these luminous objects requires the merger of two gas-rich galaxies [e.g. 3]. In theoretical work and observations of infrared luminous galaxies, the merger triggers a starburst phase which occurs concurrently with the obscured growth of the supermassive black hole [4–6]. As the obscured quasar reaches higher accretion rates, it launches powerful winds, radiation, and jets which clear out the circumnuclear material [7, 8]. This feedback coincides with the galaxy-wide decline in obscured star formation, possibly due to winds ejecting material from the host galaxy.

Testing this simple picture is mired in observational difficulties. First, quasars are not common in the local universe, and it becomes difficult to spatially resolve the central quasar from the host galaxy with increasing lookback time. Second, quasars, particularly unobscured quasars, outshine the host galaxy across a significant fraction of the electromagnetic spectrum. Isolating host galaxy emission requires reliance on spectral decomposition, which can be aided particularly by the inclusion of far-infrared observations as these are more likely to arise from the host galaxy [9].

In this talk, I discuss combining X-ray and far-IR observations in a wide-area survey to identify a rare population of “cold quasars” which do not fit neatly into the evolutionary picture outlined above.

## 2. Finding Rare Quasars

### 2.1 The Accretion History of AGN

The Accretion History of AGN is a multi-wavelength survey that assembles multiwavelength data from the 31 deg<sup>2</sup> Stripe 82X field. The X-ray observations in come from *XMM-Newton* observations in AO10 and AO13 as well as *XMM-Newton* archival pointings and *Chandra* archival pointings [10]. Stripe82X is covered by warm *Spitzer* (3.6 & 4.5  $\mu$ m only) through the *Spitzer*/HETDEX Exploratory Large Area survey, the *Spitzer* IRAC Equatorial Survey, and by *WISE* in the mid-IR. It is also covered in the near-IR by the Vista Hemisphere Survey and the UKIRT Infrared Deep Sky Survey. Stripe82X has spectroscopic redshifts from the Sloan Digital Sky Survey and dedicated programs on Palomar Observatory and Keck Observatory for 63% of the sample. From this catalog, 15.6 deg<sup>2</sup> is also fully covered by *Herschel Space Observatory* observations with the SPIRE instrument as part of the *Herschel* Stripe82 Survey [HerS; 11].

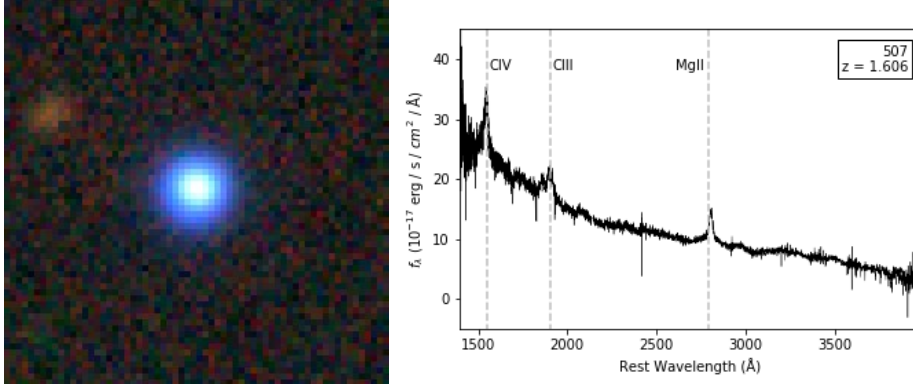


**Figure 1:** Example of a cold quasar at  $z = 1.606$  (from [12]). Left: an RGB image, where blue is the  $g$ -band filter from the DECam Legacy Survey, green is the  $r$ -band, and red is the  $z$ -band. Each side of the image is  $20''$ . The blue color indicates that this quasar is not dust reddened. All of our cold quasars are blue point sources. Right: rest frame optical SDSS spectrum with the broad lines labeled.

## 2.2 Cold Quasar Definition

I will briefly summarize the selection of the original cold quasar sample [12]. In the  $15.6 \text{ deg}^2$  region of Stripe82X with X-ray and *Herschel*/SPIRE coverage, there were 2905 X-ray detected sources. These sources spanned  $L_X = 10^{40} - 10^{46} \text{ erg/s}$  and  $z = 0 - 6$ . Of these, a mere 120 had a detection in one of the *Herschel*/SPIRE bands, due to the relative shallowness of the *Herschel* observations in this field. There are 805 unobscured quasars in the sample, according to the following criteria:

1.  $L_{2-10 \text{ keV}} > 10^{44} \text{ erg/s}$
2.  $M_B < -23$

Thirty-one unobscured quasars also have a detection in the *Herschel*/SPIRE  $250 \mu\text{m}$  band (the detection threshold is  $S_{250} \geq 30 \text{ mJy}$ ). These thirty-one sources are called cold quasars because of the substantial amount of far-IR emission arising from cold dust. The remaining 89 sources which have *Herschel*/SPIRE data but are not unobscured quasars are referred to as the *Herschel* subsample throughout.

## 3. Unique Properties of Cold Quasars

Visually, cold quasars all appear as blue point sources, and they have broad UV emission lines indicative of Type 1 AGN (Figure 1).

Measuring the optical reddening of cold quasars is an essential component to confirming that the central point source is truly unobscured. To determine the reddening,  $E(B - V)$ , we fit a model consisting of an unobscured quasar template [13] and an SMC dust model [14] to the SDSS spectra for all galaxies from the *Herschel* subsample with spectra. Figure 2 shows  $E(B - V)$  versus the absolute magnitude in the *WISE* W3 filter ( $\lambda_{\text{eff}} = 12 \mu\text{m}$ , a proxy for the amount of hot dust). The cold quasars in general have  $E(B - V) < 1$ , despite having the brightest W3 magnitudes. This demonstrates that the central region is either free from dust, or the dust has a patchy geometry.

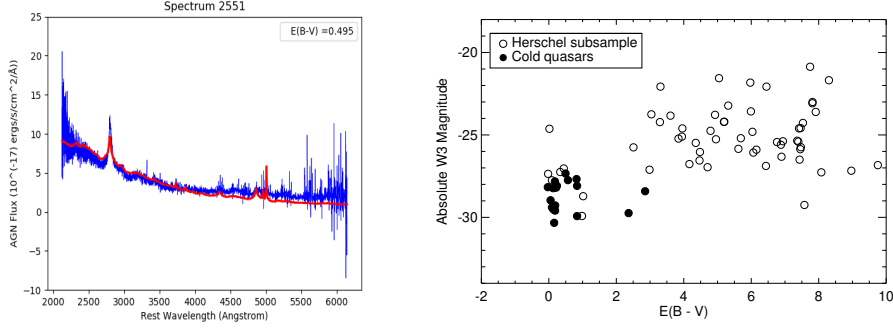


**Figure 2:** Dust reddening of cold quasars. Left: An example of how reddening was measured. We fit an unobscured quasar template, modified by SMC-like dust, to SDSS spectra to determine  $E(B - V)$ . Right: Reddening vs. absolute WISE W3 magnitude, a proxy for the hot dust. Cold quasars have low  $E(B - V)$  but bright W3 emission, indicating the substantial dust emission is not arising from the central nuclear region.

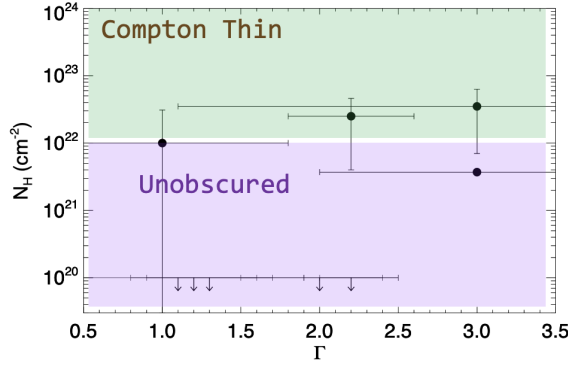


**Figure 3:** Column density,  $N_H$ , vs. photon index,  $\Gamma$  for the nine cold quasars for which we could extract an X-ray spectrum. Five sources have only an upper limit on their obscuration as indicated by the downward arrows, although uncertainties on  $\Gamma$  are still shown. The shaded regions indicate the typical definitions for classifying sources as Compton Thin and Unobscured. The cold quasars are nearly all unobscured by gas.

The other source of potential obscuration in the nuclear region is gas. Several cold quasar spectra have high enough count rates from *XMM-Newton* for a spectrum to be extracted. We fit these spectra with the NASA spectral fitter *Xspec*. For all our sources, we use a modified power law with three free parameters: intrinsic extinction ( $N_H$ ), photon index ( $\Gamma$ ), and normalization.  $\Gamma$  is restricted to a range of 1 – 3. Figure 3 shows column density as a function of photon index. There is no correlation between the parameters. All of the cold quasars have  $N_H < 10^{24}$  cm<sup>-2</sup>. Six are completely unobscured, while three fall into the Compton Thin region ( $N_H = 10^{22} - 10^{24}$  cm<sup>-2</sup>). It should be noted, however, that within the uncertainties on  $N_H$ , these sources could also be unobscured.

### 3.1 Extreme Star Formation

For the host galaxy properties of the cold quasars and *Herschel* subsample,  $M_*$ ,  $M_{\text{dust}}$ , and star formation rate (SFR) were measured using the spectral energy decomposition code SED3FIT, which fits unobscured star formation and AGN emission, both modified by dust obscuration [15].

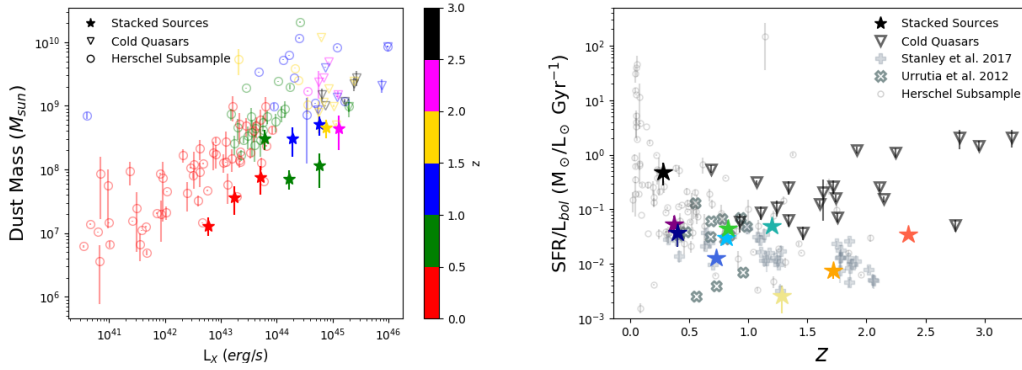


**Figure 4:** The extreme dust masses and SFRs of cold quasars (from [15]). Left:  $M_{\text{dust}}$  for the *Herschel* subsample (open circles), cold quasars (open triangles), and *Herschel*-undetected X-ray sources (stars). Cold quasars have 5 – 10 $\times$  more dust than their undetected counterparts of the same luminosity. Right:  $\text{SFR}/L_{\text{bol}}$  vs. redshift probes how much of the energy emission arises from young stars as compared with black hole accretion. Cold quasars have substantially more star formation than other quasar populations at similar redshifts.

Both the AGN and star forming components assuming an energy balance model, so that UV/optical emission that is obscured by dust is then re-radiated in the infrared. To form a comparison sample, we sorted the 2785 Stripe82X X-ray sources without a *Herschel* detection into bins of  $L_X$  and  $z$ . We stacked the *Herschel*/SPIRE positions in each bin to obtain a detection, and we averaged together the multiwavelength photometry to create an average spectral energy distributions. We used SED3FIT to decompose the average spectral energy distribution for each bin [15].

We also converted  $L_{2-10\text{keV}}$  into a bolometric luminosity,  $L_{\text{bol}}$  [12].  $L_{\text{bol}}$  is a proxy for the black hole accretion rate, assuming some radiative efficiency. Figure 4 shows  $\text{SFR}/L_{\text{bol}}$  as a function of redshift for several quasar samples, including the cold quasars.  $\text{SFR}/L_{\text{bol}}$  can be thought of as an energy budget parameter. That is, proportionally, how much of a galaxy’s emission is arising from young stars versus accretion onto a black hole? We compare the cold quasars with the *Herschel* subsample, dust obscured quasars [“red quasars” 16], optically-selected quasars [17], and the *Herschel*-undetected sample.

As can be seen, the cold quasars have substantially more star formation than every other sample at similar redshifts. (The high  $\text{SFR}/L_{\text{bol}}$  values at  $z < 0.5$  are driven by sources with  $L_X < 10^{43}$  erg/s.) In fact, [12] found that cold quasars all resided 3 – 30 $\times$  about the galaxy main sequence. This is well into the starbursting regime. Cold quasars, then, can be understood as unobscured quasars which reside in starbursting galaxies.

### 3.2 Massive Black Holes

Twelve of the original cold quasar sample were at the right redshift range to have coverage of either the MgII or  $H\beta$  emission line. We fit these with the spectral decomposition tool PyQSOFit, which measures the quasar continuum, broad, and narrow line emission. We convert the broad component of either MgII or  $H\beta$  into a black hole mass following the relations in [18]. Figure 5 shows  $M_{\bullet}$  as a function of  $M_{\star}$  for these cold quasars. We also overplot the local relation [1]. The

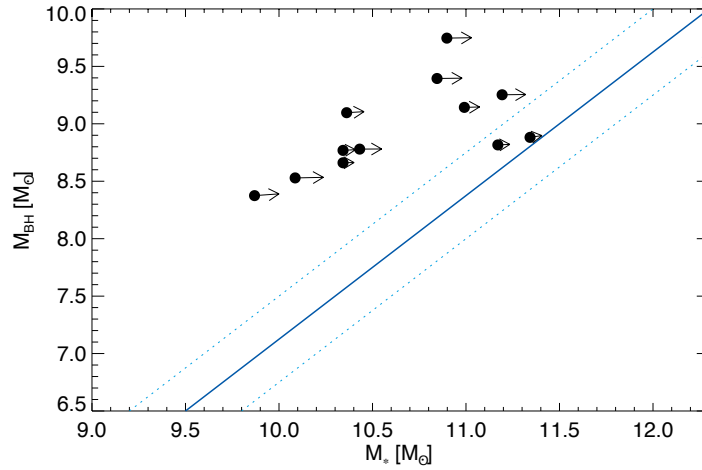


**Figure 5:** Black hole mass versus stellar mass for the cold quasars ( $z \sim 1 - 3$ ). The local relation and scatter are shown at the blue lines. The arrows indicate where each galaxy will lie after 500 Myr, if the SFR and black hole accretion rate remains constant. Cold quasars need to convert their cold gas reservoir into  $M_*$  in order to reach the local relation.

cold quasars all lie above the local relation, some substantially so. We used the black hole accretion rate (calculated from  $L_{\text{Bol}}$  and SFRs) to quantify how mass is increasing in these galaxies. The arrows indicate where each galaxy will lie after 500 Myr.  $M_*$  is increasing proportionally much faster than  $M_\bullet$ . Cold quasars will reach the local relation, only if all of the available gas is converted into stars ( $M_{\text{gas}}$  was estimated from  $M_{\text{dust}}$  assuming a constant gas-to-dust ratio). This implies that feedback cannot, by necessity, play a major role in dispelling the gas.

#### 4. Cold quasars—breaking the standard model?

Cold quasars are rare objects, as they are unobscured but have anomalously high star formation rates (SFRs) and substantial dust masses, which must be arising from a starbursting host. The high SFRs and relatively low stellar masses of cold quasars (compared with other quasar populations) do not appear consistent with the merger-driven quasar evolution scenario. In this population, the quasar phase appears to precede the starburst phase. In fact, quasar outflows may be compressing the host galaxy gas, triggering positive feedback and causing the burst of star formation. This hypothesis can be tested with resolved images of interstellar medium in the host galaxies, taken with ALMA, or by searching for quasar winds with IFU observations. Cold quasars pose an extraordinary opportunity to rethink quasar evolution.

#### References

- [1] J. Kormendy and L. C. Ho *Coevolution (Or Not) of Supermassive Black Holes and Host Galaxies*, *ARAA* **51** (2013) 511 [1304.7762].
- [2] P. Madau and M. Dickinson, *Cosmic Star-Formation History*, *ARAA* **52** (2014) 415 [1403.0007].

- [3] E. Treister, P. Natarajan, D. B. Sanders, C. M. Urry, K. Schawinski, J. Kartaltepe, *Major Galaxy Mergers and the Growth of Supermassive Black Holes in Quasars*, *Science* **328** (2010) 600 [1003.4736].
- [4] D. B. Sanders and I. F. Mirabel, *Luminous Infrared Galaxies*, *ARAA* **34** (1996) 749.
- [5] P. F. Hopkins, R. S. Somerville, L. Hernquist, T. J. Cox, B. Robertson, Y. Li, *The Relation between Quasar and Merging Galaxy Luminosity Functions and the Merger-driven Star Formation History of the Universe*, *ApJ* **652** (2006) 864 [astro-ph/0602290].
- [6] E. Treister, C. M. Urry, K. Schawinski, C. N. Cardamone, D. B. Sanders, *Heavily Obscured Active Galactic Nuclei in High-redshift Luminous Infrared Galaxies*, *ApJL* **722** (2010) 2 [1009.2501].
- [7] M. J. Page, M. Symeonidis, J. D. Vieira, et al., *The suppression of star formation by powerful active galactic nuclei*, *Nature* **485** (2012) 213 [1310.4147].
- [8] C. Ricci, B. Trakhtenbrot, M. J. Koss, et al., *The close environments of accreting massive black holes are shaped by radiative feedback*, *Nature* **549** (2017) 488 [1709.09651].
- [9] J. R. Mullaney, D. M. Alexander, A. D. Goulding, R. C. Hickox, *Defining the intrinsic AGN infrared spectral energy distribution and measuring its contribution to the infrared output of composite galaxies*, *ApJ* **414** (2011) 1082 [1102.1425].
- [10] S. M. LaMassa, C. M. Urry, N. Cappellutti, et al., *The 31 Deg<sup>2</sup> Release of the Stripe 82 X-Ray Survey: The Point Source Catalog*, *ApJ* **817** (2016) 172 [1510.00852].
- [11] M. P. Viero, V. Asboth, I. G. Roseboom, et al., *The Herschel Stripe 82 Survey (HerS): Maps and Early Catalog*, *ApJS* **210** (2014) 22 [1308.4399].
- [12] A. Kirkpatrick, C. M. Urry, J. Brewster, et al., *The Accretion History of AGN: A Newly Defined Population of Cold Quasars*, *ApJ* **900** (2020) 5 [1908.04795]
- [13] E. Glikman, T. Urrutia, M. Lacy, et al., *FIRST-2MASS Red Quasars: Transitional Objects Emerging from the Dust*, *ApJ* **757** (2012) 51 [1207.2175]
- [14] B. T. Draine, *Scattering by Interstellar Dust Grains. I. Optical and Ultraviolet*, *ApJ* **598** (2003) 1017 [astro-ph/0304060].
- [15] B. Coleman, A. Kirkpatrick, K. C. Cooke, et al., *Accretion history of AGN: Estimating the host galaxy properties in X-ray luminous AGN from  $z = 0-3$* , *MNRAS* **515** (2022) 82 [2206.06398].
- [16] T. Urrutia, M. Lacy, H. Spoon, E. Glikman, A. Petric, B. Schulz, *Spitzer Observations of Young Red Quasars*, *ApJ* **757** (2012) 125 [1208.4585].
- [17] F. Stanley, D. M. Alexander, C. M. Harrison, et al., *The mean star formation rates of unobscured QSOs: searching for evidence of suppressed or enhanced star formation*, *MNRAS* **472** (2017) 2221 [1707.05334].

- [18] M. Vestergaard and B. M. Peterson, *Determining Central Black Hole Masses in Distant Active Galaxies and Quasars. II. Improved Optical and UV Scaling Relationships*, *ApJ* **641** (2006) 689 [astro-ph/0601303].

DISCUSSION:

## DISCUSSION

**INGYIN ZAW:** Is there evidence of mergers in the cold quasars other than disturbances based on Sersic fitting?

**HERMAN MARSHALL:** How can it be that the nucleus is unobscured but there is a massive starburst with dust and gas that should obscure any X-ray source? Perhaps they are not actually related or just coincidental?

**MARIA GIOVANNA DAINOTTI's Comment:** The quasar rate versus star formation rate may not highlight some features since the sources have not been correcting for evolution and thus the trend for the quasar rate versus the star formation rate may not change.

The references to look how to correct for the evolution are the following:

Dainotti et al. 2023, arXiv: 2305.1366

Dainotti et al. 2022, ApJ, 331, 106D